"*N*-alkyl diketopyrrolopyrrole-based fluorophores for luminescent solar concentrators: effect of the alkyl chain on dye efficiency"

Jonathan Lucarelli,[a] Marco Lessi,[a] Chiara Manzini,[a] Pierpaolo Minei,[a] Fabio Bellina,[a,b] Andrea Pucci[a,b,]*

(a) Dipartimento di Chimica e Chimica Industriale, Università di Pisa, Via Moruzzi 13, 56124 Pisa, Italy
(b) INSTM, UdR Pisa, Via Moruzzi 13, 56124 Pisa, Italy
* Corresponding author: andrea.pucci@unipi.it;

Abstract

We report on the preparation of luminescent solar concentrators (LSCs) made of poly(methyl methacrylate) (PMMA) thin films doped with six new diketopyrrolopyrrole (DPP) fluorophores obtained in good yields by using simple *N*-alkylation and direct C-H arylation synthetic strategies. Spectroscopic investigations in solution and in PMMA thin films combined with photocurrent measurements revealed that the branched alkyl chains were efficient in preventing DPP segregation from the PMMA matrix thanks to their higher steric hindrance. The aromatic substituent was found to expand DPP conjugation but favoured DPP adverse aggregation, thus affecting fluorescence emission and photocurrents of PMMA films. The worthwhile combination of the appropriate alkyl chain and aromatic moieties assured to achieve optical efficiency of 6.8% that was comparable to that of PMMA LSCs of the state-of-the art (7.2%).

Keywords

Diketopyrrolopyrrole fluorophores, poly(methyl methacrylate), dye dispersion, optical efficiency, luminescent solar concentrators

1. Introduction

Since the dawning of solar power production, concentration of solar radiation has been proposed as a solution to decrease the price of photovoltaic energy. Solar concentration is achieved by collecting the sun radiation incident on a large surface and redirecting it on a smaller area, thus allowing to reduce the amount of photoactive materials, while maintaining the same power output.[1-3] The most convenient example of this approach is represented by luminescent solar concentrators (LSCs), which show several advantages such as the ability to work with diffuse light, light weight, reduced costs, and transparency.[4-7] These last features make LSCs very well suited to be implemented in modern building architectures, which make use of plenty of coloured windows and panels.[8] LSCs are thin, flat or bulk plates of highly fluorescent materials that absorb sunlight and concentrate part of the resulting fluorescence to their edges by internal reflection according to the refractive index of the host material. The photoactive elements are organic dyes, luminescent nanoparticles or Eu^{3+} complexes dispersed in a transparent polymer matrix such as poly(methyl methacrylate) (PMMA).[8-10] The solar radiation is thus conveniently transmitted to PV cells at their edges, even with a cloudy sky. Nevertheless, current LSC-PV devices achieve too low power conversion efficiencies, being strongly plagued by a multitude of unfavourable processes that hinder their ability to deliver light to PV cells, in particular re-absorption of light emitted by luminescent species. [8, 11] [5, 12-21] Notably, the maximum power conversion efficiency of 7.1% was recorded for a LSC-PV device based on the perylene derivative Lumogen F Red 305, whose recently quotation (~7,500 €/kg, BASF) might limit the worldwide distribution of the LSC technology.[21]

Although LSC-PV devices that exploit the optical features of organic luminophors are well documented,[5, 12, 14, 16, 22-24] alternative and effective red-emitting fluorophores to perylene derivatives are not available yet. Recent research has been focused on the use of (dicyanomethylene)-2-t-butyl-6-(1,1,7,7-tetramethyljulolidyl-9-enyl)-4H-pyran (DCJTB)

fluorophore (Figure 1),[17, 25-27], but the optical performances of the derived PMMA-based LSC appeared still lower than the state-of-the art.[26]

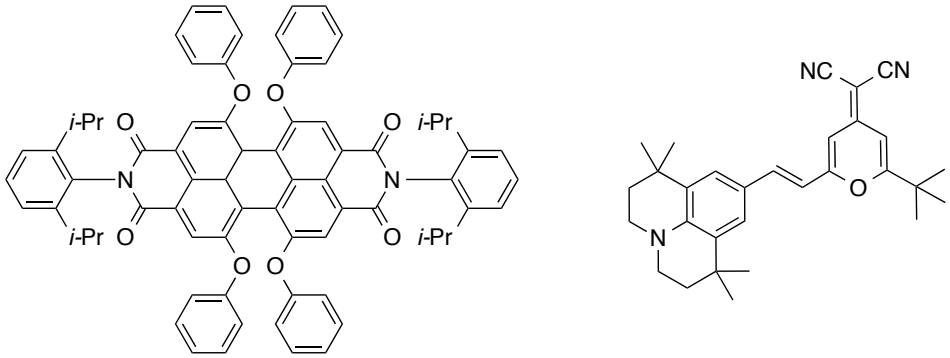

Figure 1. Chemical structures of Lumogen F Red 305 and DCJTB

Surprisingly, fluorophores based on the diketopyrrolopyrrole (DPP) core structure are, to the best of our knowledge, still ignored as dopants for LSC. DPPs are structurally based on the π-conjugated 2,5-dihydropyrrolo[4,3-c]pyrrolo-1,4-dione dilactam moiety, which is easily functionalized by electrophilic and nucleophilic reactions. Functional DPPs are well-known compounds with high fluorescence quantum yields and exceptional thermal and photostability, which make them excellent building blocks for many applications.[28, 29] For example, DPPs are widely used as pigments in paints, varnishes, and high-quality printing[30, 31] and exhibit outstanding semiconducting properties for advanced organic field-effect transistors (OFETs) and organic light-emitting diodes (OLEDs).[32-34]

Notable is the fact that the modification of the DPP structure, both on the nitrogen atoms and on the aryl groups on 3 and 6 positions, has a great impact on the solubility of these compounds and on their absorption and fluorescence properties.[35] For example, the introduction of alkyl substituents onto the nitrogen atoms of DPP results in significant improvement in the DPP solubility, as they are no longer able to form intermolecular hydrogen bonds.[36] The modification of aryl groups at positions 3 and 6 of the DPP core causes significant bathochromic shifts in the absorption and emission maxima and provides intense fluorescence bands near 600 nm.[28] Recent papers

demonstrated that the position, length, and bulkiness of these alkyl chains strongly affect the aggregation behaviour of these materials in solid state, thus impact their electronic properties.[37-39] However, the influence of DPP aggregation on material fluorescence has not yet been addressed fully and it merits further study.

Herein, we report on the impact of different *N*-alkyl chains on the optical behaviour in solution and in PMMA film of six diketopyrrolopyrrole-based fluorophores, i.e., compounds **1a-c** and **2a-c** (Figure 2) for the preparation of high performance LSC.

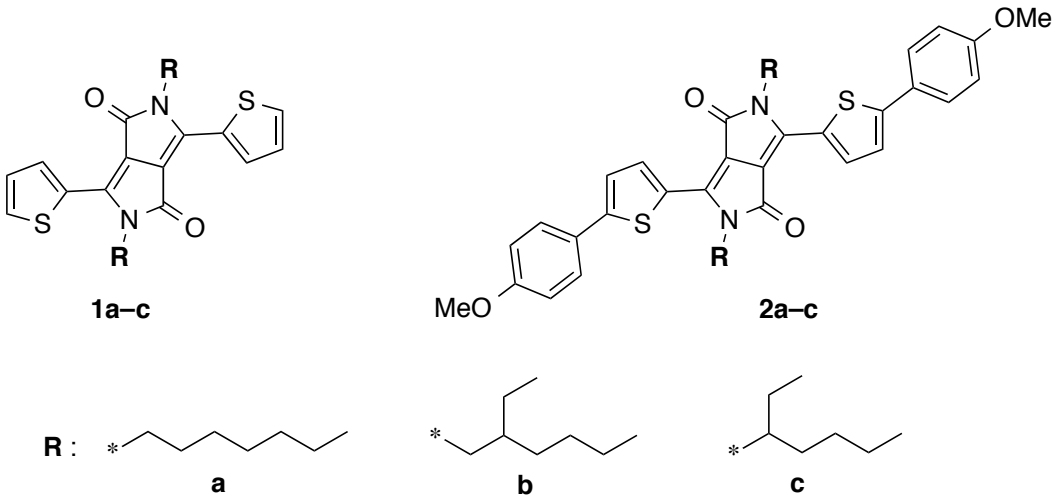

Figure 2. Chemical structures of the synthesized fluorophores: 2,5-dioctyl-3,6-di(thiophen-2-yl)-2,5-dihydropyrrolo[3,4-*c*]pyrrole-1,4-dione (**1a**); 2,5-*bis*(3-ethylheptyl)-3,6-di(thiophen-2-yl)-2,5-dihydropyrrolo[3,4-*c*]pyrrole-1,4-dione (**1b**); 2,5-*bis*(2-ethylhexyl)-3,6-di(thiophen-2-yl)-2,5-dihydropyrrolo[3,4-*c*]pyrrole-1,4-dione (**1c**); 3,6-*bis*(5-(4-methoxyphenyl)thiophen-2-yl)-2,5-dioctyl-2,5-dihydro pyrrolo[3,4-*c*]pyrrole-1,4-dione (**2a**); 2,5-*bis*(3-ethylheptyl)-3,6-*bis*(5-(4-methoxyphenyl)thiophen-2-yl)-2,5-dihydropyrrolo[3,4-*c*]pyrrole-1,4-dione (**2b**) and 2,5-*bis*(2-ethylhexyl)-3,6-*bis*(5-(4-methoxyphenyl)thiophen-2-yl)-2,5-dihydropyrrolo[3,4-*c*]pyrrole-1,4-dione (**2c**)

Thin-film LSC devices were prepared by the dispersion of the synthesized fluorophores in poly(methyl methacrylate) (PMMA) films coated over high optical quality glass slab. The LSC optical efficiencies were discussed in terms of the effect provided by the three different alkyl chains in relation to the aryl substitution of the DPP core, and compared to that measured for LSC devices with the same geometry and containing Lumogen F Red 305.

2. Experimental part

2.1 Materials

Unless otherwise stated, all reactions were performed under argon by standard syringe, cannula and septa techniques. 3-Ethyl-1-iodoheptane (**4b**) was prepared according to a literature procedure.[40] All the other commercially available reagents and solvents were used as received. Poly(methyl methacrylate) (PMMA, Aldrich, *Mw* = 350,000 g/mol, acid number <1 mg KOH/g).

*2.2. 2,5-Dioctyl-3,6-di(thiophen-2-yl)-2,5-dihydropyrrolo[3,4-c]pyrrole-1,4-dione (**1a**)*

This compound was synthesized according to a literature procedure.[41] 3,6-Di(thiophen-2-yl)pyrrolo[3,4-*c*]pyrrole-1,4(2*H*,5*H*)-dione (**3**) (0.45 g, 1.5 mmol) and K_2CO_3 (0.83g, 6.0 mmol) were added to the reaction vessel. The reaction vessel was fitted with a silicon septum, evacuated, and back-filled with argon. This sequence was repeated twice. Anhydrous DMF (16 mL) was added under a stream of argon, and the resulting mixture was stirred at 120 °C for 1h. Then, 1-iodooctane (**4a**) (1.44 g, 6.0 mmol) was added in one portion, and the mixture was stirred at 120 °C for 24 h. After cooling to room temperature, the reaction mixture was poured into ice-cold water (100 mL), and extracted with CH_2Cl_2 (4x25 ml). The organic fractions were collected, dried over Na_2SO_4, filtered, and concentrated at reduced pressure. The residue was purified by flash chromatography on silica gel with a mixture of CH_2Cl_2 and petroleum ether (1:1) as eluent. The chromatographic fractions containing the required compound were collected and concentrated at reduced pressure to give **1a** as a dark pink solid (0.46 g, 58 % yield): mp 141-143 °C [Lit: mp 143 °C].[41] ^{1}H NMR (400 MHz $CDCl_3$) δ (ppm) 8.93 (dd, J = 3.9, 1.2 Hz, 2H), 7.63 (dd, J = 5.1, 1.2 Hz, 2H), 7.28 (dd, J = 5.1, 3.9 Hz, 2H), 4.07 (m, 4 H), 1.74 (m, 4 H), 1.33 (m, 20 H), 0.87 (t, J = 6.1 Hz, 6H). The spectral properties of this compound are in agreement with those previously reported.[41]

*2.3. 2,5-Bis(3-ethylheptyl)-3,6-di(thiophen-2-yl)-2,5-dihydropyrrolo[3,4-c]pyrrole-1,4-dione (**1b**)*

This compound was synthesized in a similar fashion to compound **1a**, substituting 3-ethyl-1-iodoheptane (**4b**) for 1-iodooctane (**4a**). The crude reaction mixture was purified by flash

chromatography on silica gel with a mixture of CH_2Cl_2 and petroleum ether (1:1) as eluent. The chromatographic fractions containing the required compound were collected and concentrated at reduced pressure to give **1b** as a dark pink solid (0.46 g, 55 % yield): mp 134-136°C. ^{1}H NMR (400 MHz, $CDCl_3$) δ (ppm) 8.90 (dd, J = 3.9, 1.2 Hz, 1H), 7.65 (dd, J = 5.1, 1.1 Hz, 1H), 7.30 (dd, J=5.1, 3.9 Hz, 2 H), 4.10 (m, 4 H), 1.70 (m, 4 H), 1.38 (m, 18 H), 0.91 (t, J = 6.9 Hz, 12H). ^{13}C NMR (100 MHz, $CDCl_3$): δ = 161.5, 140.2, 135.2, 130.6, 129.9, 128.7, 108.1, 41.0, 37.6, 33.6, 32.9, 29.0, 26.0, 23.2, 14.3, 11.0 ppm. HRMS (ESI) m/z found $[M + H]^+$ 553.2919; $C_{32}H_{44}N_2O_2S_2$ requires $[M + H]^+$ 553.2917.

*2.4. 2,5-Bis(2-ethylhexyl)-3,6-di(thiophen-2-yl)-2,5-dihydropyrrolo[3,4-c]pyrrole-1,4-dione (**1c**)*

This compound was synthesized in a similar fashion to compound **1a**, substituting 2-ethylhexyl bromide (**4c**) for 1-iodooctane (**4a**). The crude reaction mixture was purified by flash chromatography on silica gel with a mixture of CH_2Cl_2 and petroleum ether (1:1) as eluent. The chromatographic fractions containing the required compound were collected and concentrated at reduced pressure to give **1c** as a dark pink solid (0.19 g, 24 % yield): mp 127 °C. ^{1}H NMR (400 MHz, $CDCl_3$) δ (ppm) 8.91 (dd, J = 3.9, 1.2 Hz, 2H), 7.65 (dd, J = 5.0, 1.2 Hz, 2H), 7.29 (dd, J=5.0, 3.9 Hz, 2 H), 4.05 (m, 4 H), 1.88 (m, 2 H), 1.33 (m, 16 H), 0.89 (m, 12 H). The spectral properties of this compound are in agreement with those previously reported.[42]

*2.5. General procedure for the palladium-catalyzed direct arylation of 2,5-dialkyl-3,6-di(thiophen-2-yl)-2,5-dihydropyrrolo[3,4-c]pyrrole-1,4-diones **1a-c** with 4-bromoanisole*

According to a modified literature procedure,[43] a 2,5-*bis*-alkyl-3,6-di(thiophen-2-yl)-2,5-dihydropyrrolo[3,4-*c*]pyrrole-1,4-dione (**1a**, **1b** or **1c**) (0.12 mmol), anhydrous K_2CO_3 (0.3 mmol, 41 mg), pivalic acid (0.036 mmol, 3.67 mg), $Pd(OAc)_2$ (0.006 mmol, 1.35 mg) were suspended into anhydrous DMA (2 mL) in a 25 mL two-neck round flask and degassed for 10 minutes under argon atmosphere. Then, 1-bromo-4-methoxybenzene (0.3 mmol, 56,1 mg) was added, and the resulting dark purple mixture was stirred at 110 °C for 24h. It was cooled to room temperature, then washed

with water (100 ml) and extracted with CH_2Cl_2 (3x100 ml). The organic fractions were collected, dried over Na_2SO_4, filtered and concentrated at reduced pressure. The residue was purified by flash chromatography on silica gel. This procedure was used to prepare compounds **2a–c**.

*2.5.1. 3,6-Bis(5-(4-methoxyphenyl)thiophen-2-yl)-2,5-dioctyl-2,5-dihydropyrrolo[3,4-c]pyrrole-1,4-diones **2a***

The crude reaction product, which was obtained by Pd-catalyzed reaction of **1a** with 4-bromoanisole, was purified by flash chromatography on silica gel with a mixture of CH_2Cl_2 and petroleum ether (8:2) as eluent to give **2a** (44 mg, 50 %) as a dark purple solid: mp 250–252 °C. ^{1}H NMR(400 MHz, $CDCl_3$): δ = 8.94 (d, J = 4.2 Hz, 2H), 7.62 (m, 4H), 7.3 (d, J = 4.2 Hz, 2H), 6.95 (m, 4 H), 4.11 (m, 4H), 3.86 (s, 6H), 1.79 (m, 4H), 1.37 (m, 20 H), 0.87 (m, 6H) ppm. ^{13}C NMR (100 MHz, $CDCl_3$): δ = 161.5, 169.5, 150.1, 139.5, 136.9, 128.1, 127.7, 126.2, 123.8, 114.8, 108.0, 55.6, 42.4, 32.0, 30.2, 29.4, 27.1 (2C), 22.8, 14.2 ppm. HRMS (ESI) m/z found $[M + H]^+$ 737.3410; $C_{44}H_{52}N_2O_4S_2$ requires $[M + H]^+$ 737.3441.

*2.5.2. 2,5-Bis(3-ethylheptyl)-3,6-bis(5-(4-methoxyphenyl)thiophen-2-yl)-2,5-dihydropyrrolo[3,4-c]pyrrole-1,4-diones **2b***

The crude reaction product, which was obtained by Pd-catalyzed reaction of **1b** with 4-bromoanisole, was purified by flash chromatography on silica gel with a mixture of CH_2Cl_2 and petroleum ether (7:3) as eluent to give **2b** (50.5 mg, 55 %) as a dark purple solid: mp 215–217 °C. ^{1}H NMR(400 MHz, $CDCl_3$): δ = 8.96 (d, J = 4.2 Hz, 2H), 7.63 (m, 4H), 7.39 (d, J = 4.2 Hz, 2H), 6.97 (m, 4 H), 4.15 (t, J = 8.4 Hz, 4H), 1.76 (m, 4H), 1.42 (m, 18 H), 0.83 (m, 12H) ppm. ^{13}C NMR (100 MHz, $CDCl_3$): δ = 161.5, 160.1, 150.0, 139.6, 136.8, 128.0, 127.7, 126.3, 123.8, 114.8, 108.1, 55.6, 41.2, 37.8, 33.7, 33.0, 29.2, 26.1, 23.3, 14.3, 11.1 ppm. HRMS(ESI) m/z found $[M+Na]^+$ 787.3558; $C_{46}H_{56}N_2O_4S_2$ requires $[M+Na]^+$ 787.3574.

*2.5.3. 2,5-Bis(2-ethylexyl)-3,6-bis(5-(4-methoxyphenyl)thiophen-2-yl)-2,5-dihydropyrrolo[3,4-c]pyrrole-1,4-diones **2c***

The crude reaction product, which was obtained by Pd-catalyzed reaction of **1c** with 4-bromoanisole, was purified by flash chromatography on silica gel with a mixture of CH_2Cl_2 and petroleum ether (8:2) as eluent to give **2b** (41 mg, 45 %) as a dark purple solid: mp 214–216 °C. ^{1}H NMR(400 MHz, $CDCl_3$): δ = 8.94 (d, J = 4.1 Hz, 2 H), 7.62 (m, 4 H), 7.36 (d, J = 4.1 Hz, 2 H), 6.96 (m, 4 H), 4.08 (m, 4 H), 3.86 (s, 6 H), 1.95 (m, 2 H), 1.34 (m, 16 H), 0.89 (m, 12H). The spectral properties of this compound are in agreement with those previously reported.[44]

2.6 Preparation of polymer films for optical studies

Different dye/PMMA thin films were prepared by drop casting, i.e. pouring 0.8 mL chloroform solution containing 30.5 mg of the polymer and the proper amount of dye to obtain concentrations in the range 0.1–2.0 wt.% on 35x50 mm area over a glass surface. The glass slides were cleaned with chloroform and immerged in 6 M HCl for at least 12 h, then they were rinsed with water, acetone and isopropanol and dried for 8 h at 120 °C. Solvent evaporation was performed on a warm hot plate (about 30 °C) and in a closed environment. The film thickness was measured by a Starrett micrometer to be 25±5 μm. The PMMA films were easily removed with a spatula after immersion in water so that they can be stored for successive measurements and comparison by attaching them on 50x50x3 mm optically pure glass substrate (Edmund Optics Ltd BOROFLOAT window 50x50 TS) with a high-purity silicone oil with a refractive index comparable to PMMA and glass (i.e., poly(methylphenyl siloxane), 710 fluid, Aldrich, refractive index n = 1.5365). Absorption and emission properties of such devices showed negligible differences with the freshly prepared ones.

2.7 Apparatus and Methods

Melting points were recorded on a hot-stage microscope (Reichert Thermovar). Fluka precoated silica gel PET foils were used for TLC analyses. Purifications by flash chromatography were

performed using silica gel Merck 60 (particle size 0.040-0.063 mm). NMR spectra were recorded at room temperature at 400 MHz (^{1}H) and 100 MHz (^{13}C) and were referred to TMS or to the residual protons of deuterated solvents.

ESI-Q/ToF flow injection analyses (FIA) were carried out using a 1200 Infinity HPLC (Agilent Technologies, USA), coupled to a Jet Stream ESI interface (Agilent) with a Quadrupole-Time of Flight tandem mass spectrometer 6530 Infinity Q-TOF (Agilent Technologies). Two sets of eluents were used: 100% MeOH or 85% H2O and 15% acetonitrile, both added with 1% formic acid. The flow rate was 0.2 mL/min. Injection volume: 3 μL. The ESI operating conditions were: drying gas (N2, purity >98%): 350 °C and 10 L/min; capillary voltage 4.5 KV; nebuliser gas 35 psig; sheath gas (N2, purity >98%): 375 °C and 11 L/min.

Absorption spectra were recorded at room temperature on a Perkin-Elmer Lambda 650 spectrometer. Fluorescence spectra were measured at room temperature on a Horiba Jobin-Yvon Fluorolog®-3 spectrofluorometer and equipped with a 450 W xenon arc lamp, double-grating excitation and single-grating emission monochromators. The fluorescence of dye/PMMA films were recorded by using the Solid-Sample Holder and collecting the front-face emission at 30°.

The fluorescence quantum yield (Φ_f) in chloroform was determined at room temperature relative to Rhodamine B ($\Phi^s_f = 0{,}5$ in ethanol) using the following relation:[45]

$$\Phi_X = \Phi_{ST}\left(\frac{Grad_X}{Grad_{ST}}\right)\left(\frac{\eta_X^2}{\eta_{ST}^2}\right)$$

Where the subscripts ST and X are standard and dye respectively, Grad the gradient from the plot of integrated fluorescence intensity vs absorbance for different solutions of standard and dyes. In order to minimise re-absorption effects absorbances never exceed 0.1 at and above the excitation wavelength. η is the refractive index of the solvent, i.e. Refractive indexes of ethanol and chloroform were assumed 1.361 for ethanol and 1.446 for chloroform.[46]

Photocurrent measurements

A proper apparatus was build and composed by a plywood wooden box 15x15x30 cm with walls 1.5 cm thick. A removable cover hosting a housing for a solar lamp is present at the top. During the measurement a solar lamp TRUE-LIGHT® ESl E27 20W was used. Two 50x3 mm slits were carved out at 5 cm from the bottom of the box to exactly fit the LSC systems (dimensions 50x50x3 mm) so that the minimum amount of light would come out during the measurement conditions. On the outer side of the slit, a set of three 1x1 cm photodiodes (THORLABS FDS1010 Si photodiode, with an active area of 9.7 x 9.7 mm and high responsivity (A/W) in the spectral range of 400–1100 nm) connected in parallel fashion was placed and coupled to a multimeter (KEITHLEY Mod. 2700) for photocurrent measuring. In order to collect a more intense and stable output signal, both the photodiodes and the multimeter are connected to an amplifier, realized in laboratory, following the specifications given by THORLABS. The measurement procedure comprehends a 20 minutes warm-up for the lamp, in order to reach its maximum power output. After this time, the current intensity can be measured every minute, for a total of five minutes.

Efficiency measurement using a PV-cell

A different set of LSC samples was prepared to measure the concentration efficiency attaching a Si-PV cell (IXYS SLMD121H08L mono solar cell 86x14 mm, with a solar cell efficiency of 22% and a fill factor > 70%) to one edge of the sample. This set of samples was made covering the full 50x50 area of the previously introduced optically pure glass slabs with a 24±5 μm dye/PMMA thick film. One edge of the LSC was connected to a Si–based PV cell masked to cover just the LSC edge (50x3 mm) using silicone grease while the remaining edges were covered with an aluminum tape. These devices where then placed over a white poly(ethylene terephthalate) scattering sheet (Microcellular® MCPET reflective sheet, ERGA TAPES Srl) and placed about 20 cm under a solar lamp (TRUELIGHT® ESL E27 20W, with a correlated color temperature of 5500 K). The efficiency is reported as η_{opt}, which is the ratio between the short circuit current of the PV cell

attached the LSC edges under illumination of a light source (I_{LSC}) and the short circuit current of the bare cell put perpendicular to the light source (I_{SC}).

3. Results and discussion

3.1 Synthesis of DPP-based fluorophores

The six DPP-based fluorophores **1a–c** and **2a–c** were prepared by known synthetic procedures starting from commercially available 2,5-dihydro-1,4-dioxo-3,6-dithienylpyrrolo [3,4-c]-pyrrole (**3**). At first, **3** was reacted with the appropriate alkyl halide **4a–c** in DMF solution at 120 °C in the presence of K_2CO_3 for 24h. The resulting deep red-colored 2,5-dialkylsubstituted DPP derivatives **1a–c** were then regioselectively arylated at the C5 position of the two thiophene rings with 4-methoxyphenyl bromide in the presence of $Pd(OAc)_2$ as the precatalyst, K_2CO_3 as the base, and pivalic acid (PivOH) in DMA.[44, 47] The required DPP fluorophores **3a–c** were isolated after 24 h at 110 °C in 50, 55, and 45 % yield, respectively (Scheme 1).

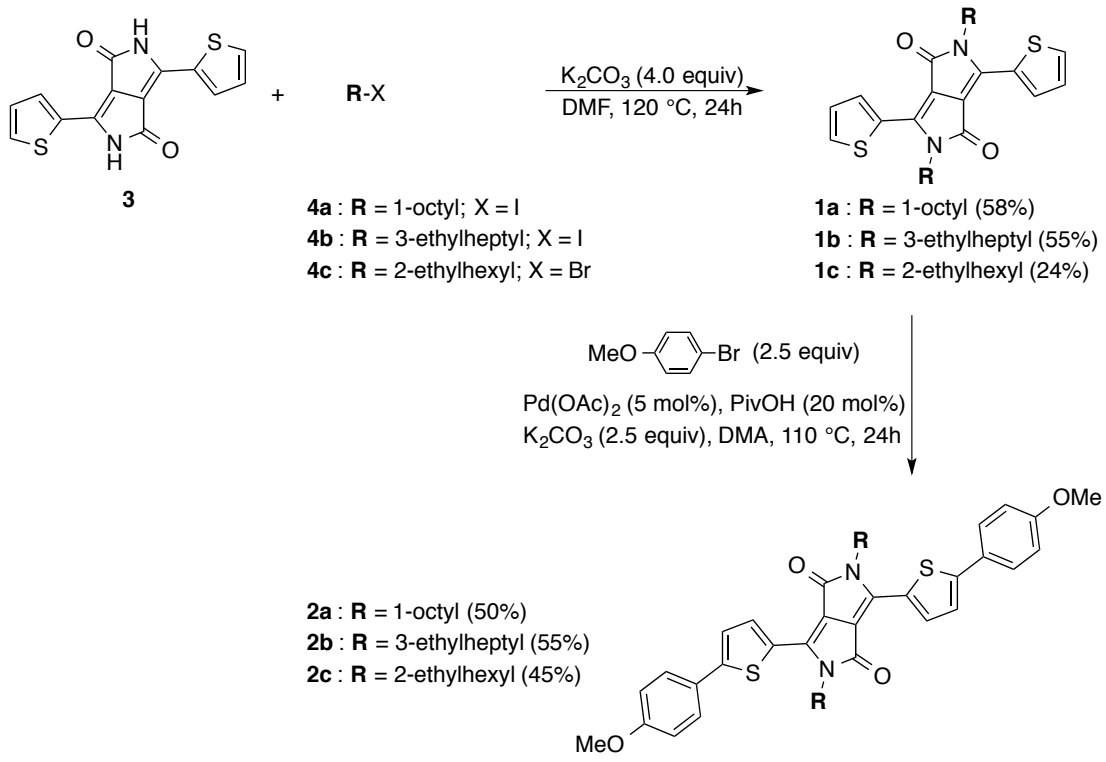

Scheme 1. Synthesis of DPP fluorophores **1a–c** and **2a–c**

3.2 Optical properties of DPP-based fluorophores

The optical properties of the prepared DPP compounds were examined by UV-vis absorption and photoluminescent spectroscopies, and the main results were collected in Table 1.

Table 1. Spectroscopic data of DPP compounds: absorption and emission maxima (λ_{max}), molar extinction coefficients (ε_{max}), and fluorescence quantum yields (Φ_f)

	Absorption		**Fluorescence**	
Compound	λ_{max} (nm)	$10^{-4}\ \varepsilon_{max}$ ($M^{-1}cm^{-1}$)	λ_{max} (nm)	Φ_f (%)
1a	549	5.4	563	48
1b	549	9.0	564	52
1c	548	5.0	563	56
2a	605	10.0	630	52
2b	568 and 605	13.0	630	53
2c	568 and 606	10.2	631	55

Figure S1 shows the absorption spectra of all DPP compounds in $CHCl_3$ solution. **1a-c** fluorophores display similar absorption profiles with strong low energy bands at around 513 and 550 nm attributed to donor-acceptor charge transfer transitions, and high energy bands near 320 nm due to localised π–π transitions.[44] Fluorophores **2a-c** show the same band structure, but bathochromically shifted to between 500 and 650 nm, with the two maxima positioned around 570 and 607 nm, respectively. The introduction of the 4-methoxyphenyl substituent on the thiophene rings lowers in energy the onset of the absorption and promotes the molar extinction coefficient rising according to the enlargement of the π-electron system in these molecules. [48] The different alkyl chain attached on the nitrogen atoms does not significantly affect the absorption profile in $CHCl_3$ solution. Conversely, the ethylheptyl moiety in compounds **1b** and **2b** contributes in amplifying the molar extinction coefficient, possibly due to the increased solubility of the compound in the solvent (Table 1).[39, 49]

The fluorescence of the DPP compounds in $CHCl_3$ solution exhibits a mirror image relation with respect to the corresponding absorption (Figure S2). Fluorophores **1a-c** display a similar profile with a large fluorescence characterised by a main emission at 564 nm and a smaller contribution at around 610 nm due to the vibronic structure. Fluorophores **2a-c** show a significant bathochromic

shift of the emission maximum, with a larger band centred at 631 nm, and the vibronic contribution at around 680 nm. This phenomenon confirms the effect provided by the 4-methoxyphenyl donor group on the fluorophore π-conjugation and emission characteristics. Quantum yields higher than 50% were calculated in $CHCl_3$ and no significant differences between these values are observed (Table 1).

3.3 Optical properties of DPP-based fluorophores in PMMA

Owing to the aforementioned properties, that is good quantum yields and emission shifted to the red portion of the electromagnetic spectrum of light, DPP compounds were dispersed at different concentrations (0.1–2.0 wt.%) in a transparent and totally amorphous polymer matrix such as PMMA. These concentrations were selected to realize homogeneous polymer films of a thickness of 24 ± 5 μm with optical and morphological features that are not impacted by spurious effects stemming from high fluorophore content such as phase-separation and dye segregation at the film surface. Aim of this approach was the determination of the optical properties of the derived thin films in terms of their potential use as LSC.

In detail, the linear *n*-octyl chain on compound **1a** was the less efficient in preventing the aggregation of the fluorophore molecules, thus the limit concentration for a homogeneous film was set at 1.4 wt.%. The two branched ethylheptyl and ethylhexyl chains allowed to increase this limit, i.e. 1.8 wt.% for **1b** and 2.0 wt.% for **1c**, respectively, thanks to their higher steric hindrance which makes interactions between DPP cores more difficult to occur. This trend was also confirmed for the **2a-c** fluorophores (0.4, 0.8 and 1 wt.%, respectively), even if the stronger π-π stacking interactions between DPP molecules due to the higher conjugation rendered the effect of the branched alkyl functionalities less effective.

The optical properties of **1a-c** and **2a-c** fluorophores dispersed in PMMA films follow a similar trend as a function of dye content. In figure 3, the main absorption and emission characteristics of

1c/PMMA and **2c**/PMMA films are displayed as the most representative, whereas reporting in figures S3 and S4 those of the other samples.

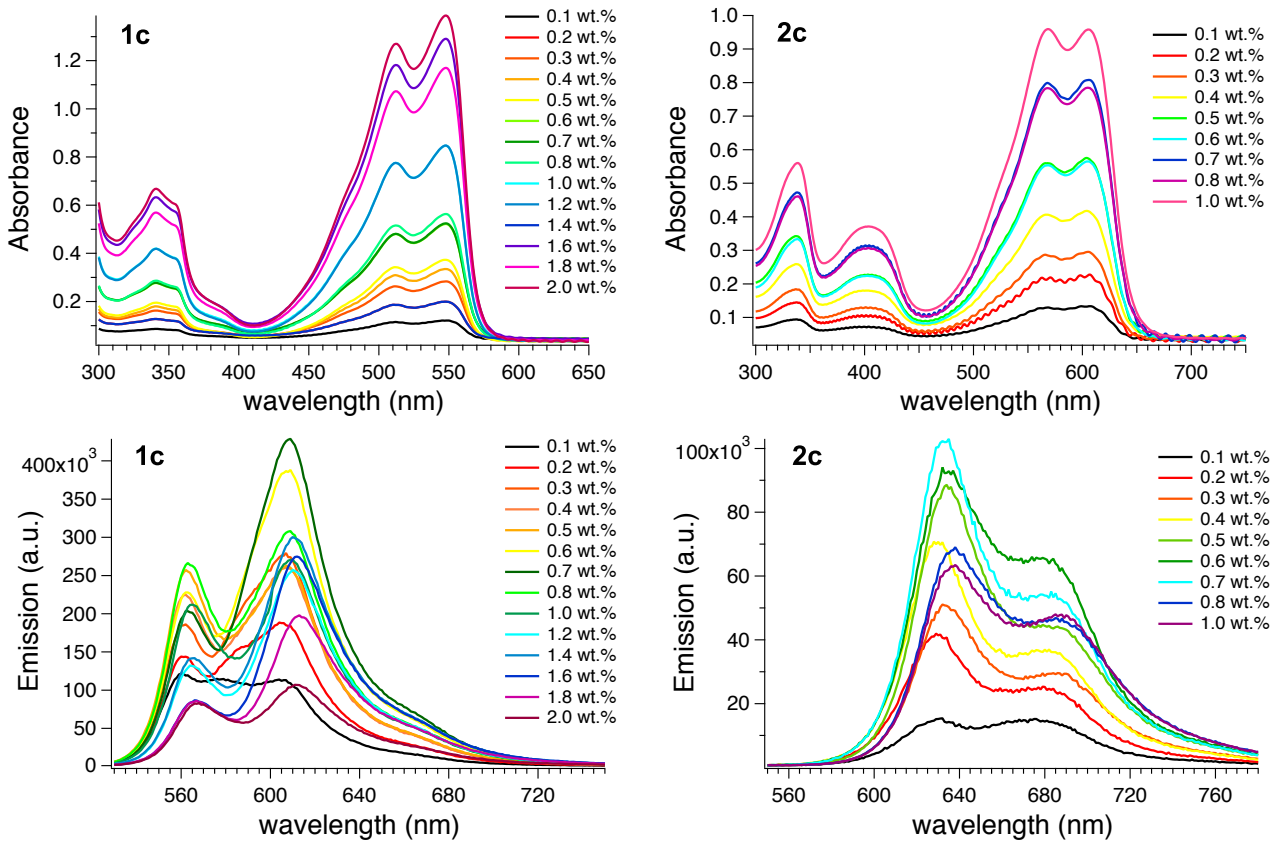

Figure 3. 1c/PMMA films: absorption (up, left) and emission (down, left) spectra as a function of dye content (wt.%); **2c**/PMMA films: absorption (up, right) and emission (down, right) spectra as a function of dye content (wt.%). Film thickness = 15 ± 5 μm; λ_{exc} = 525 nm

The absorption spectra of **1c**/PMMA and **2c**/PMMA films show large absorption bands with two maxima positioned at 513-550 nm and at 570-607 nm, respectively. These values are equivalent to those collected in $CHCl_3$ solution due to the similar polarity indexes of the dispersing media.[50] Differently from solution, the absorption spectra of PMMA films level off at the highest concentration possibly due to saturation phenomena, which start causing dye segregation from the polymer matrix but without promoting the emersion of any significant band due to DPP aggregates. Conversely, the emission spectra of **1c**/PMMA and **2c**/PMMA films strongly differ from those in solution, particularly in the case of **1a-c** compounds (see also figure S4). According to literature,

DPP-based molecules with thiophene rings display the typical monomeric emission band at around 560 nm flanked by an intense non-structured emission band at longer wavelengths (>600 nm), which emerges with fluorophore concentration.[51] This behaviour, together with the absence of typical ground-state aggregates in the absorption spectra, is ascribed to the formation of excimers (excited dimers) that originate from interactions between the excited state of the molecule and the ground state of the same molecule.[52] The excimers stabilise the excited state causing photons emission at lower energy, thus overall reducing the spectral overlap between the absorption and emission bands. Being the excimer band predominant over the monomeric emission, Stokes shift increases (i.e., from about 15 nm to 60 nm) and brings the emission maximum to wavelengths higher than 600 nm. The progression of the excimer band at the expenses of the monomer contribution was clearly observed by plotting the ratio between excimer and monomer emission intensities (I_{605}/I_{560}) with **1c** content (Figure S5). Nevertheless, the excimer increasing with dye content occurred up to a threshold concentration (i.e. 1.4 wt.% for **1c**/PMMA film), above which the emission experienced a substantial decreasing being higher the probability to find quenching centres through energy transfer between closely spaced pairs.[53]

In stark contrast to the aforementioned case, the **2c**/PMMA film shows emission features equivalent to those collected in $CHCl_3$ solution with fluorescence bands pointed at 630 and 680 nm and Stokes shift of about 25 nm. The emission intensity increased with fluorophore content up to 0.7 wt.%, above which fluorescence quenching occurred. For highly conjugated DPP fluorophores such as **2a–c**, the photoluminescence is effectively quenched in the solid state due to the aggregation among molecules. These strong interactions provide the sites for non-radiative recombination and significantly reduce the probability of radiative emission. In other words, aggregates in PMMA from the **2a–c** serie appeared non luminescent with respect to those from **1a–c**, which in turn impacted on the overall fluorescence emission of the derived films. To confirm such behaviour, the fluorescence emission intensity was plotted vs. absorbance for **1c**/PMMA and **2c**/PMMA films, in

order to reveal possible loss of the absorbed photons via non-radiative pathways (Figure S6).[54] In detail, the emission intensity of PMMA films was found to increase linearly with the absorbance up to 0.8 wt.% and 0.7 wt.% of **1c** and **2c**, respectively, indicating a negligible effect of dissipation phenomena. Conversely, when the concentration was increased further, a deviation from linearity was observed, suggesting that dissipative phenomena occur. It is worth noticing that for **1c**/PMMA films the fluorescence emission intensity levels off up to 1.2 wt.% of **1c,** before dropping to minimum values. Conversely, for **2c**/PMMA films, an evident decrease of the luminescent response occurs just after the linear regime (i.e., for **2c** content higher than 0.8 wt.%), thus confirming the non-emissive nature of the **2c** aggregates.

3.4 Photocurrent measurements and data analysis of DPP-based fluorophores in PMMA

In order to assess the performances as Luminescent Solar Concentrators (LSCs), an optically pure 50x50x3 mm glass was coated with DPP fluorophore/PMMA films with a thickness of 15 ± 5 μm. In Figure 3, an example of LSC obtained by coating a thin layer of **1c**/PMMA (Figure 4a) and of **2c**/PMMA (Figure 4b) are reported.

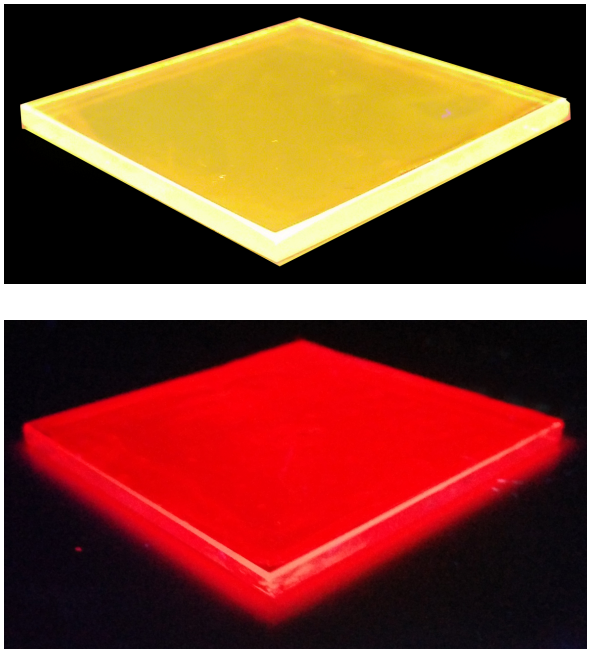

(a)

(b)

Figure 3. Optically pure 50x50x3 mm glass coated with (a) **1c**/PMMA film and with (b) **2c**/PMMA film. Film thickness = 15 ± 5 μm; λ_{exc} = 366 nm

Notably, **1c**/PMMA and **2c**/PMMA LSCs emit light colors such as yellow and red, respectively, in agreement with the position of the fluorescence bands in the photoluminescent spectra reported in figure 3.

Photocurrent measurements were accomplished with a home-built apparatus[55] (see experimental part) by using a set of three 1x1 cm photodiodes assembled in parallel fashion. Photodiodes are ideal for measuring light sources in LSC emission range by converting the optical power to an electrical current, allowing for a fast, precise and reproducible response even with different sets of samples. This approach was used to study the best working conditions for different DPP/PMMA LSC systems since the response curves of the photodiodes and the utilized PV module do not differ significantly. For example, the photocurrents measured for a set of samples based on **1c**/PMMA and **2c**/PMMA thin film are reported in figure 5.

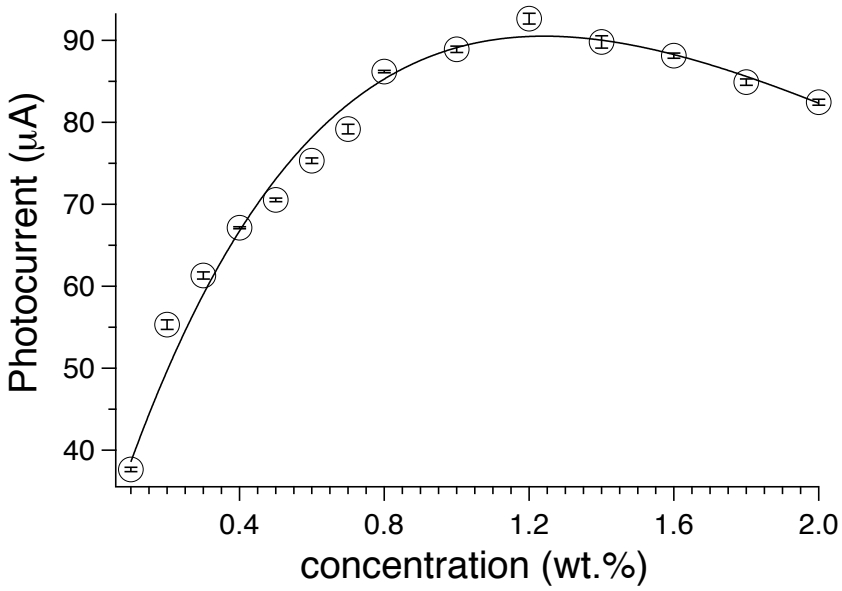

(a)

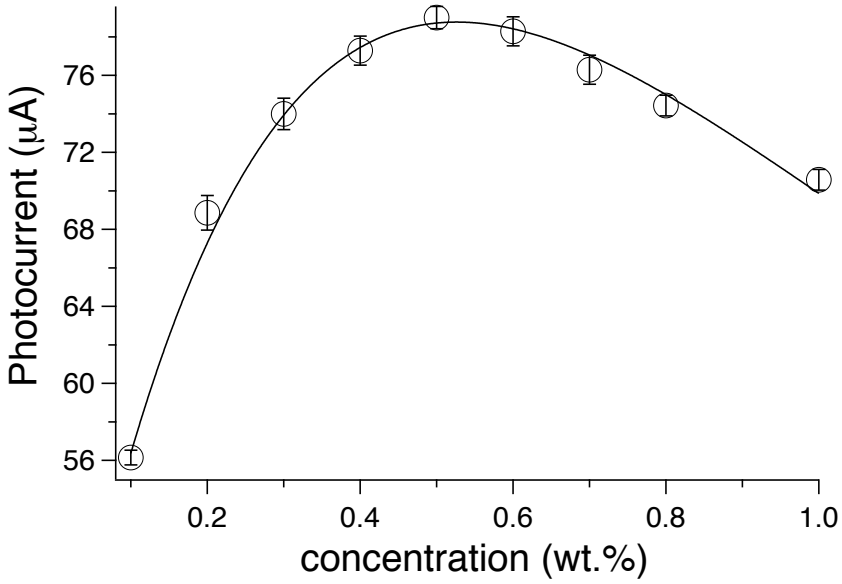

(b)

Figure 5. Photocurrent variation of (a) **1c**/PMMA and (b) **2c**/PMMA thin films with different dye content (wt.%), with a thickness of 15±1 μm and deposited on a 50x50x3 mm optically pure glass substrate. The curves were fitted with eq. 1 with the following parameters: for **1c**/PMMA, ε' = 142±7, μ_{opt} = 0.81±0.02, D = 25±2; for **2c**/PMMA, ε' = 208±8, μ_{opt} = 1.89±0.03, D = 39±1.

The current intensity is found to increase up to a maximum peaked at about 1.2 wt.% of **1c** and 0.5 wt.% of **2c**, after that a slow decreasing occurs due to the presence of dissipative phenomena of the emission response. This result agrees well with the fluorescence behaviour of the respective **1c**/PMMA and **2c**/PMMA thin films (Figure 3 and S6), being the latter less emissive than the former at the highest fluorophore content.

Notably, the photocurrent behaviour fits quite well with eq. 1:

$$\eta_{opt} = \varepsilon' \cdot c \cdot e^{-\mu_{opt} \cdot c} + D \quad \text{(eq. 1)}$$

where η_{opt} is a term proportional to the current generated by photodiods, c is the concentration of the dye in wt.%, and ε' and μ_{opt} are two empirical constants defined as:

$$\varepsilon' \propto h \cdot e^{-\bar{l}} \quad \text{(eq. 2)}$$

$$\mu_{opt} \propto \mu''(QY, p) \cdot \bar{l} \quad \text{(eq. 3)}$$

where h is the thickness of the thin film, $\bar{l}$ is the mean path length of the radiation in the optical system and μ'' is a term depending on both QY and the probability of fluorescence re-absorption

(p), being greater at high p and low QY. D is an empirical constant added since even an empty system of transparent material (c = 0) is capable of trapping some light by means of surface and bulk defects due to scattering phenomena. Eq. 1 was inspired by the work of Goezberger[11] who proposed in 1977 an effective method to evaluate LSC efficiency. Both ε' and μ_{opt} must be considered as completely empirical since even the most accurate estimations require strong approximations. Nevertheless, the determination of how they affect the final η_{opt} is straightforward for determining the LSC performances. Notably, ε' is a coefficient related to the absorption properties of the dye/polymer system, whereas μ_{opt} combines all the fluorescence quenching mechanisms due to the dye. An optimal dye/polymer system should therefore present a high ε' and a small μ_{opt} so that the maximum efficiency is shifted to higher concentrations and the curve steadily rises under the influence of the linear part (eq. 1). A complete and exhaustive determination of eq. 1 was recently reported in literature by our group.[55]

The fitting parameters, reported in table 2, were compared to those recently gathered for PMMA films with the same thickness but containing the Lumogen Red F 305 (LR, Figure 1), selected as reference as it is considered the state-of-the-art in dyes for LSC applications.[56]

Table 2. Fitting parameters of the photocurrent data measured for **1a-c**/PMMA, **2a-c**/PMMA and **LR**/PMMA[56] films.

Entry	ε'	μ_{opt}	D
1a/PMMA	138±6	1.07±0.01	14±1
1b/PMMA	213±10	1.29±0.02	28±2
1c/PMMA	142±7	0.81±0.02	25±2
2a/PMMA	297±10	3.11±0.07	14±1
2b/PMMA	413±31	3.09±0.14	8±3
2c/PMMA	208±8	1.89±0.03	39±1
LR/PMMA	140	0.45	20

The fitting parameters collected in table 2 show an increase in the *ε'* values going from the **1a-c** fluorophores, to the 4-methoxyphenyl functionalised **2a-c** compounds. This fact indicates that the functionalised fluorophores are capable to reach the highest photocurrent values at a lower concentration regime, thanks to their higher molar extinction coefficient due to the enlarged π-electron system (see table 1). These values are comparable and often superior to those reported for **LR**/PMMA systems, thus indicating that DPP compounds have great potentialities as fluorophores for LSC applications.

Conversely, the smaller μ_{opt} values gathered from **1a-c** with respect to **2a-c** are addressed to the larger Stokes shifts of the former fluorophores, i.e. 62 against 25 nm, which is a fundamental feature that prevents dye self-absorption and efficiency losses. Moreover, it is clear the role provided by the branched 2-ethylhexyl functionalities in reducing dissipative phenomena thanks to its superior ability to maintain **1c** and **2c** fluorophores better dispersed within PMMA. Indeed, the 3-ethylheptyl chains reveals less performing in preventing efficiency losses caused by dye aggregation, possibly due to the larger distance between alkyl ramification and DPP nucleus. It is worth noting that **1c**/PMMA shows μ_{opt} value close to that gathered from the **LR**/PMMA system (i.e., 0.81±0.02 against 0.45), thus confirming the use of DPP dyes as effective substitutes of perylene-based fluorophores in LSC.

On the other hand, D values resulted to be quite similar for all the dye/PMMA systems, thus

suggesting that the contribution of non–fluorescent trapping is more or less the same for samples with the same thickness.

1a-c/PMMA and **2a-c**/PMMA films with the highest photocurrents were analysed by using a Si-based PV cell attached to one edge of the concentrator, as described in the experimental section. The optical efficiency η_{opt} (Table 3) was evaluated from the concentration factor C, which is the ratio between the short circuit current measured in the case of the cell over the LSC edge (I_{LSC}) and short circuit current of the bare cell when perpendicular to the light source (I_{SC}) (eq. 4):

$$\eta_{opt} = \frac{I_{LSC}}{I_{SC} \cdot G} \qquad \text{(eq. 4)}$$

where G is the geometrical factor (in our case, G = 13.3), which is the ratio between the area exposed to the light source and the collecting area. The data collected were compared to that gathered from LSC based on **LR** in the same range of fluorophore concentration and geometrical factor.

Table 3. Optical efficiencies (η_{opt}) calculated for **1a-c**/PMMA, **2a-c**/PMMA and compared to that of **LR**/PMMA with similar dye content and geometrical factor[56]

Entry	wt.%	η_{opt} (%)
1a/PMMA	0.8	6.1
1b/PMMA	0.9	5.9
1c/PMMA	1.2	6.8
2a/PMMA	0.4	5.3
2b/PMMA	0.3	5.4
2c/PMMA	0.5	6.1
LR/PMMA	1.4	7.2

Notably, η_{opt} increases for both DPP series **1** and **2** on going from fluorophores with linear *n*-octyl chains to compounds bearing branched 2-ethylhexyl moieties, in agreement with the photodiodes measurements. The 2-ethylhexyl group helps in keeping DPP nuclei well separated, thus acting as an effective compatibilizing tool for DPP fluorophores in PMMA.

As far as the effect of the 4-methoxyphenyl group is concerned, expanded π-electron system would favour higher efficiency values being the fluorophore emission superimposes the wavelenght range

of PV cell maximum efficiency. Conversely, **2a-c** show lower values than **1a-c**, possibly due to the larger Stokes shifts of the latter fluorophores which helps in reducing dissipative disexcitation phenomena. Accordingly, the **1c**/PMMA system shows the η_{opt} maximum of 6.8 that is comparable to that of LSC based on **LR**/PMMA thin film (η_{opt} = 7.2%) collected for similar fluorophore content (1.4 wt.%).[56]

The capability to retain the fluorescence intensity after continuous light irradiation is a fundamental requisite for fluorophores in LSC applications. Photostability tests were eventually carried out by continuously irradiating a 0.25 cm^2 area of **1c**/PMMA and **2c**/PMMA films at their excitation wavelengths (i.e. 550 nm and 607 nm, respectively) with a 450 W Xe arc lamp under aerobic conditions.[35] Notably, **1c**/PMMA and **2c**/PMMA films retained respectively the 95% and 99% of their fluorescence, after 60 min of continuous excitation, thus indicating great photostability,[28] which makes DPP fluorophores a viable alternative to perylene derivatives for LSC applications.

Conclusions

We have shown that DPP fluorophores once embedded into PMMA, confers to the resulting thin films optical efficiencies, which make them suitable for the preparation of LSCs. DPP fluorophores based on the donor-acceptor-donor skeleton were prepared by *N*-alkylation and direct C-H arylation. Linear *n*-octyl chain and the aromatic substituent (4-methoxyphenyl) on the thiophene rings were found to adversely affect DPP fluorescence due to their tendency to promote DPP aggregation, which in turn limited fluorophore dispersion within PMMA. By contrast, the branched 2-ethylhexyl chains and the unsubstituted thiophene moieties allowed to obtain the best performing DPP fluorophore in PMMA thin film in terms of dye compatibility, fluorescence emission and photocurrent intensities. In light of these special features, DPP/PMMA LSC system yielded maximum optical efficiencies (η_{opt}) of 6.8%, which were found comparable to that gathered from LSC based on LR in the same range of fluorophore concentration and geometrical factor. The

performances were attributed to the larger Stokes shift of DPP bearing unsubstituted thiophene moieties that prevented loss of efficiencies due to self-absorption. Future approaches for η_{opt} enhancement should adopt new synthetic strategies aimed at limiting DPP extensive aggregation while maintaining the emission maxima in the range of the highest quantum efficiency of the PV cell (> 600 nm). Considering the easy preparation and excellent photostability, all findings consistently support the effective use of the DPP fluorophores in the realization of high performance LSCs.

Acknowledgements

The research leading to these results has received funding from MIUR-FIRB (RBFR122HFZ) and in part from the Università di Pisa under PRA 2015 (project No. 2015_0038). ERGA TAPES Srl and BASF Italia S.p.A are kindly acknowledged for providing some free samples of "Microcellular® MCPET reflective sheet" and Lumogen Red F 305, respectively.

References

[1] Debije M. Renewable energy Better luminescent solar panels in prospect. Nature. 2015;519(7543):298-9.

[2] Sawin JL. Renewables Global Status Report. Renewable Energy Policy Network for the 21th Century. Renewable Energy Policy Network for the 21th Century ed. Paris: Renewable Energy Policy Network for the 21th Century; 2014.

[3] van Sark WGJHM. Luminescent solar concentrators - A low cost photovoltaics alternative. Renewable Energy. 2013;49(0):207-10.

[4] Bailey ST, Lokey GE, Hanes MS, Shearer JDM, McLafferty JB, Beaumont GT, et al. Optimized excitation energy transfer in a three-dye luminescent solar concentrator. Solar Energy Materials and Solar Cells. 2007;91(1):67-75.

[5] Sanguineti A, Sassi M, Turrisi R, Ruffo R, Vaccaro G, Meinardi F, et al. High Stokes shift perylene dyes for luminescent solar concentrators. Chemical Communications. 2013;49(16):1618-20.

[6] ten Kate OM, Kraemer KW, van der Kolk E. Efficient luminescent solar concentrators based on self-absorption free, Tm2+ doped halides. Solar Energy Materials & Solar Cells. 2015;140:115-20.

[7] Meinardi F, McDaniel H, Carulli F, Colombo A, Velizhanin KA, Makarov NS, et al. Highly efficient large-area colorless luminescent solar concentrators using heavy-metal-free colloidal quantum dots. Nature Nanotechnology. 2015;10(10):878-85.

[8] Debije MG, Verbunt PPC. Thirty Years of Luminescent Solar Concentrator Research: Solar Energy for the Built Environment. Advanced Energy Materials. 2012;2(1):12-35.

[9] Tonezzer M, Gutierrez D, Vincenzi D. Luminescent solar concentrators - state of the art and future perspectives. Solar Cell Nanotechnology. 2014:293-315.

[10] Lim YS, Kee SY, Lo CK. Recent research and development of luminescent solar concentrators. Solar Cell Nanotechnology. 2014:271-91.

[11] Goetzberger A, Greube W. Solar energy conversion with fluorescent collectors. Appl Phys. 1977;14(2):123-39.

[12] Turrisi R, Sanguineti A, Sassi M, Savoie B, Takai A, Patriarca GE, et al. Stokes shift/emission efficiency trade-off in donor-acceptor perylenemonoimides for luminescent solar concentrators. Journal of Materials Chemistry A: Materials for Energy and Sustainability. 2015;3(15):8045-54.

[13] Meinardi F, Colombo A, Velizhanin KA, Simonutti R, Lorenzon M, Beverina L, et al. Large-area luminescent solar concentrators based on 'Stokes-shift-engineered' nanocrystals in a mass-polymerized PMMA matrix. Nature Photonics. 2014;8(5):392-9.

[14] Griffini G, Levi M, Turri S. Thin-film luminescent solar concentrators: A device study towards rational design. Renewable Energy. 2015;78:288-94.

[15] Zhao Y, Meek GA, Levine BG, Lunt RR. Near-Infrared Harvesting Transparent Luminescent Solar Concentrators. Advanced Optical Materials. 2014;2(7):606-11.

[16] Benjamin WE, Veit DR, Perkins MJ, Bain E, Scharnhorst K, McDowall S, et al. Sterically Engineered Perylene Dyes for High Efficiency Oriented Fluorophore Luminescent Solar Concentrators. Chemistry of Materials. 2014;26(3):1291-3.

[17] Currie MJ, Mapel JK, Heidel TD, Goffri S, Baldo MA. High-Efficiency Organic Solar Concentrators for Photovoltaics. Science. 2008;321(5886):226-8.

[18] Daorta SF, Liscidini M, Andreani LC, Scudo P, Fusco R. THEORETICAL STUDY OF MULTILAYER LUMINESCENT SOLAR CONCENTRATORS USING A MONTE CARLO APPROACH. 26th European Photovoltaic Solar Energy Conference and Exhibition. Hamburg2011.

[19] Desmet L, Ras AJM, de Boer DKG, Debije MG. Monocrystalline silicon photovoltaic luminescent solar concentrator with 4.2% power conversion efficiency. Opt Lett. 2012;37(15):3087-9.

[20] Goldschmidt JC, Peters M, Bosch A, Helmers H, Dimroth F, Glunz SW, et al. Increasing the efficiency of fluorescent concentrator systems. Solar Energy Materials and Solar Cells. 2009;93(2):176-82.
[21] Slooff LH, Bende EE, Burgers AR, Budel T, Pravettoni M, Kenny RP, et al. A luminescent solar concentrator with 7.1% power conversion efficiency. physica status solidi (RRL) – Rapid Research Letters. 2008;2(6):257-9.
[22] Griffini G, Brambilla L, Levi M, Del Zoppo M, Turri S. Photo-degradation of a perylene-based organic luminescent solar concentrator: Molecular aspects and device implications. Solar Energy Materials and Solar Cells. 2013;111(0):41-8.
[23] Han BG, Kim JS. The luminescent solar concentrators with the H-aggregate of perylene diimide dye imbedded into PMMA. Fibers and Polymers. 2015;16(4):752-60.
[24] ter Schiphorst J, Kendhale AM, Debije MG, Menelaou C, Herz LM, Schenning APHJ. Dichroic Perylene Bisimide Triad Displaying Energy Transfer in Switchable Luminescent Solar Concentrators. Chem Mater. 2014;26(13):3876-8.
[25] Zhou W, Wang M-C, Zhao X. Poly(methyl methacrylate) (PMMA) doped with DCJTB for luminescent solar concentrator applications. Sol Energy. 2015;115:569-76.
[26] Zhou W, Wang M-C, Zhao X. The properties of PMMA/DCJTB thin-film luminescent solar concentrator with various thicknesses. Sol Energy. 2015;120:419-27.
[27] El Mouedden Y, Ding B, Song Q, Li G, Nguyen H, Alameh K. A cost-effective, long-lifetime efficient organic luminescent solar concentrator. J Appl Phys. 2015;118(1):015502/1-/5.
[28] Kaur M, Choi DH. Diketopyrrolopyrrole: brilliant red pigment dye-based fluorescent probes and their applications. Chem Soc Rev. 2015;44(1):58-77.
[29] Qu S, Tian H. Diketopyrrolopyrrole (DPP)-based materials for organic photovoltaics. Chemical Communications. 2012;48(25):3039-51.
[30] Faulkner EB, Schwartz RJ. High performance pigments: John Wiley & Sons, 2009.
[31] Kaur M, Choi DH. Diketopyrrolopyrrole: brilliant red pigment dye-based fluorescent probes and their applications. Chemical Society Reviews. 2015;44(1):58-77.
[32] Chandran D, Lee K-S. Diketopyrrolopyrrole: a versatile building block for organic photovoltaic materials. Macromolecular Research. 2013;21(3):272-83.
[33] Lenz R, Wallquist O. DPP chemistry—continuous innovation. Surface Coatings International Part B: Coatings Transactions. 2002;85(1):19-26.
[34] Ciardelli F, Bertoldo M, Bronco S, Pucci A, Ruggeri G, Signori F. The unique optical behaviour of bio-related materials with organic chromophores. Polym Int. 2013;62(1):22-32.
[35] Andrew TL, Swager TM. Reduced photobleaching of conjugated polymer films through small molecule additives. Macromolecules. 2008;41(22):8306-8.
[36] Lee OP, Yiu AT, Beaujuge PM, Woo CH, Holcombe TW, Millstone JE, et al. Efficient Small Molecule Bulk Heterojunction Solar Cells with High Fill Factors via Pyrene-Directed Molecular Self-Assembly. Advanced Materials. 2011;23(45):5359-63.
[37] Qu S, Tian H. Diketopyrrolopyrrole (DPP)-based materials for organic photovoltaics. Chem Commun 2012;48(25):3039-51.
[38] Ciardelli F, Ruggeri G, Pucci A. Dye-containing polymers: methods for preparation of mechanochromic materials. Chemical Society Reviews. 2013;42(3):857-70.
[39] Pucci A, Tirelli N, Ruggeri G, Ciardelli F. Absorption and emission dichroism of polyethylene films with molecularly dispersed push-pull terthiophenes. Macromolecular Chemistry and Physics. 2005;206(1):102-11.
[40] Meager I, Ashraf RS, Mollinger S, Schroeder BC, Bronstein H, Beatrup D, et al. Photocurrent Enhancement from Diketopyrrolopyrrole Polymer Solar Cells through Alkyl-Chain Branching Point Manipulation. Journal of the American Chemical Society. 2013;135(31):11537-40.

[41] Tamayo AB, Tantiwiwat M, Walker B, Nguyen T-Q. Design, Synthesis, and Self-assembly of Oligothiophene Derivatives with a Diketopyrrolopyrrole Core. The Journal of Physical Chemistry C. 2008;112(39):15543-52.
[42] Naik MA, Venkatramaiah N, Kanimozhi C, Patil S. Influence of Side-Chain on Structural Order and Photophysical Properties in Thiophene Based Diketopyrrolopyrroles: A Systematic Study. The Journal of Physical Chemistry C. 2012;116(50):26128-37.
[43] Zhang J, Kang D-Y, Barlow S, Marder SR. Transition metal-catalyzed C-H activation as a route to structurally diverse di(arylthiophenyl)-diketopyrrolopyrroles. Journal of Materials Chemistry. 2012;22(40):21392-4.
[44] Hendsbee AD, Sun J-P, Rutledge LR, Hill IG, Welch GC. Electron deficient diketopyrrolopyrrole dyes for organic electronics: synthesis by direct arylation, optoelectronic characterization, and charge carrier mobility. Journal of Materials Chemistry A. 2014;2(12):4198-207.
[45] Brouwer AM. Standards for photoluminescence quantum yield measurements in solution (IUPAC Technical Report). Pure and Applied Chemistry. 2011;83(12):2213-28.
[46] Lide D, Haynes W. CRC handbook of chemistry and physics: a ready-reference book of chemical and physical data-/editor-in-chief, David R. Lide; ass. ed. WM" Mickey" Haunes: Boca Raton, Fla: CRC, 2009.
[47] Liu S-Y, Shi M-M, Huang J-C, Jin Z-N, Hu X-L, Pan J-Y, et al. C-H activation: making diketopyrrolopyrrole derivatives easily accessible. Journal of Materials Chemistry A. 2013;1(8):2795-805.
[48] Kirkus M, Wang L, Mothy Sb, Beljonne D, Cornil Jrm, Janssen RAJ, et al. Optical Properties of Oligothiophene Substituted Diketopyrrolopyrrole Derivatives in the Solid Phase: Joint J- and H-Type Aggregation. The Journal of Physical Chemistry A. 2012;116(30):7927-36.
[49] Donati F, Pucci A, Cappelli C, Mennucci B, Ruggeri G. Modulation of the Optical Response of Polyethylene Films Containing Luminescent Perylene Chromophores. J Phys Chem B 2008;112(12):3668-79.
[50] Minei P, Koenig M, Battisti A, Ahmad M, Barone V, Torres T, et al. Reversible vapochromic response of polymer films doped with a highly emissive molecular rotor. Journal of Materials Chemistry C. 2014;2(43):9224-32.
[51] Liu Y, Tao X, Wang F, Shi J, Sun J, Yu W, et al. Intermolecular Hydrogen Bonds Induce Highly Emissive Excimers:‚Äâ Enhancement of Solid-State Luminescence. The Journal of Physical Chemistry C. 2007;111(17):6544-9.
[52] B. Valeur MNBB-S. Molecular Fluorescence Principles and Applications - 2nd edition: Wiley-VCH, 2013.
[53] Carlotti M, Gullo G, Battisti A, Martini F, Borsacchi S, Geppi M, et al. Thermochromic polyethylene films doped with perylene chromophores: experimental evidence and methods for characterization of their phase behaviour. Polymer Chemistry. 2015;6(21):4003-12.
[54] Pucci A, Pavone M, Minei P, Munoz-Garcia AB, Fanizza E, Cimino P, et al. Cost-effective Solar Concentrators based on Red Fluorescent Zn(II)-Salicylaldiminato Complex. RSC Advances. 2016;6:17474-82.
[55] Carlotti M, Fanizza E, Panniello A, Pucci A. A fast and effective procedure for the optical efficiency determination of luminescent solar concentrators. Sol Energy. 2015;119:452-60.
[56] Carlotti M, Ruggeri G, Bellina F, Pucci A. Enhancing optical efficiency of thin-film luminescent solar concentrators by combining energy transfer and stacked design. Journal of Luminescence. 2016;171:215-20.

Graphical Abstract (for review)